Journal of Power Sources 196 (2011) 601–613

Contents lists available at ScienceDirect

Journal of Power Sources

journal homepage: www.elsevier.com/locate/jpowsour

Review

A review of polymer electrolyte membrane fuel cell stack testing

M. Miller[a,b], A. Bazylak[a,*]

[a] Microscale Energy Systems Transport Phenomena Laboratory, Department of Mechanical and Industrial Engineering, University of Toronto, 5 King's College Road, Toronto, Ontario, Canada M5S 3G8
[b] Sustainable Energy Engineering, KTH Department of Energy Technology, Royal Institute of Technology, 10044 Stockholm, Sweden

ARTICLE INFO

Article history:
Received 12 June 2010
Received in revised form 23 July 2010
Accepted 26 July 2010
Available online 4 August 2010

Keywords:
Polymer electrolyte membrane fuel cell
PEMFC
Stack testing
Fuel cell performance

ABSTRACT

This paper presents an overview of polymer electrolyte membrane fuel cell (PEMFC) stack testing. Stack testing is critical for evaluating and demonstrating the viability and durability required for commercial applications. Single cell performance cannot be employed alone to fully derive the expected performance of PEMFC stacks, due to the non-uniformity in potential, temperature, and reactant and product flow distributions observed in stacks. In this paper, we provide a comprehensive review of the state-of-the art in PEMFC testing. We discuss the main topics of investigation, including single cell vs. stack-level performance, cell voltage uniformity, influence of operating conditions, durability and degradation, dynamic operation, and stack demonstrations. We also present opportunities for future work, including the need to verify the impact of stack size and cell voltage uniformity on performance, determine operating conditions for achieving a balance between electrical efficiency and flooding/dry-out, meet lifetime requirements through endurance testing, and develop a stronger understanding of degradation.

Contents

* Corresponding author. Tel.: +1 416 946 5031; fax: +1 416 978 7753.
E-mail address: abazylak@mie.utoronto.ca (A. Bazylak).

0378-7753/$ – see front matter © 2010 Elsevier B.V. All rights reserved.
doi:10.1016/j.jpowsour.2010.07.072

1. Introduction

The polymer electrolyte membrane fuel cell (PEMFC) is a promising technology due to its high power density, low operating temperatures, low local emissions, quiet operation, and fast start-up and shutdown [1]. However, currently PEMFCs are primarily employed for research and demonstration applications due to remaining barriers of reliability, endurance, and cost [1] that hinder their widespread commercial adoption.

Extensive fundamental experimental investigations of single cell PEMFC performance have been conducted over the past several decades, whereas stack-level investigations have received less attention. Single cell research is primarily focused on material properties and transport behaviour, including membrane electrode assembly (MEA) materials [2–6], bipolar plate design [4,7–9], MEA durability and degradation [10–14], contamination [15], water management [16–20], and thermal management [21–23]. Stack-level research has been primarily focused on macroscopic issues, such as performance and durability, with studies aimed to characterize stack-level behaviour and verify semi-empirical models.

Fuel cells tend to perform differently when arranged in stacks than compared to single cells [19,24–30]. In addition to the increased power capability and fuel conversion efficiency possible with a PEMFC stack [24], the stack also tends to exhibit non-uniformity in cell voltages (across the stack) [25,26], temperatures [27], and reactant/product concentrations in the flow channels [28]. The degradation mechanisms associated with liquid water accumulation also affect stack durability [19]. Water and thermal management strategies required for stacks must accommodate the non-uniform distributions of potential, temperature and reactant/product concentrations, which are not necessarily observed at the single cell level.

In the last decade, experimental PEMFC stack performance has been investigated in a number of areas, including single cell vs. stack performance [24,29–37], individual cell voltage uniformity [25,28,31,38–65], influence of operating conditions on performance [22,24,29,32,38–44,66–83], performance analysis through a variety of electrochemical methods [20,25,26,30,33–35,40,45–48,66–70,84–96], lifetime (endurance) testing and degradation [19,30,32,45,46,49–52,67,68,71,72,84–88,97–106], dynamic testing [1,10,14,31,32,42,46,51,67,70,73,84,97–99,107–132], and stack field trials (demonstrations) [98,100,101,133–170]. Due to the proprietary nature of commercial testing, reports of stack testing in the field tend to include more general commentaries on performance and less quantitative data than those regarding laboratory trials, which typically include more highly controlled variables and parametric studies.

In this literature review we will provide a current overview of PEMFC stack-level testing. The main contributions will be presented, and future opportunities for stack research will be discussed.

2. Stack-level testing

2.1. Single cell vs. stack-level investigations

In PEMFC investigations, an important distinction should be made between a single cell and a stack. While valuable insight can be gained from investigating single cells, they are typically run in controlled testing environments. However, PEMFC stacks consist of multiple cells assembled together to meet the power demands of a variety of commercial applications, such as portable electronics and transportation. As a result of the increased size, voltage, and power capacity of a stack, additional technical considerations must be addressed. Stacks require a gas manifold to facilitate a uniform supply of reactants to all cells, a system for removal of product water and heat, and efficient electrical contacts between cells [30]. The parallel feeding of reactants and cooling medium can lead to uneven reactant flow, voltage, and temperature distributions across the stack [28,38], and the increased electrical resistance due to serial cell connections can cause performance losses [29]. Proper flow distribution, cooling plate design, and end plate design are important for achieving high performance [33].

A pertinent question regarding PEMFC stacks is to determine how well stack performance can be predicted through the linear scaling of single cell behaviour. The possibility of scaling up from a single cell to a stack has been demonstrated through the observation of similar polarization curves for single cells and stacks [24,32,34]. As shown in Fig. 1, Bonnet et al. [32] found comparable polarization curves for both a single cell and a 5-cell stack before and after operation in driving cycle conditions for 550 h. Chu and Jiang [24] also found similar polarization curves for their single cell and 30-cell stack at steady-state conditions. A scale-up investigation was also undertaken by Bonville et al. [34], who found that the polarization curve for a higher temperature 4-cell stack was similar to that of a single cell.

Other studies resulted in disagreement between single cells and stack polarization curves. Urbani et al. [29] tested both a single cell and 5-cell stack to compare their performance at standard conditions at 80 °C, low gas pressure, and low platinum (Pt) loading. Fig. 2 shows the performance decrease observed by Urbani et al. [29] when moving from a single cell to a 5-cell stack. At 0.4 A cm^{-2}, the performance of the stack was lower by 8% (0.270 W cm^{-2} for the single cell vs. 0.248 W cm^{-2} for the stack). They attributed this to parasitic losses caused by a non-uniform distribution of reactants in the stack and increased electrical resistance. Weng et al. [33] also compared a single cell and a 4-cell stack, finding lower power density in the stack than the single cell, especially above

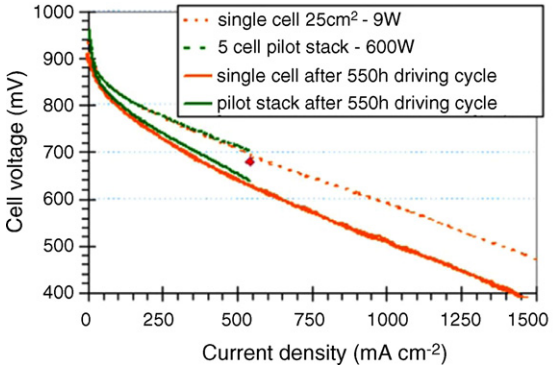

Fig. 1. Comparison between experimentally determined polarization curves for a single cell and 5-cell stack, before and after a 550 h driving cycle, reported by Bonnet et al. [32].
Reprinted from [32] with permission from Elsevier.

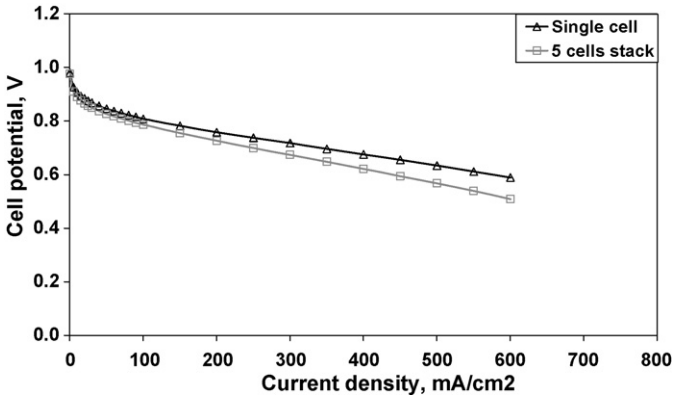

Fig. 2. Comparison between experimentally determined polarization curves for single cell and 5-cell stack operation, reported by Urbani et al. [29].
Reprinted from [29] with permission from The International Journal of Hydrogen Energy.

0.6 A cm^{-2}. They attributed this performance loss to increased ohmic resistance, increased levels of water flooding, and uneven fuel distribution in the stack.

There have been investigations that indicate single cell performance alone is not sufficient to predict the performance of a stack. Chu and Jiang [24] found that the open-circuit potential, Tafel slope, and DC resistance of a stack were equal to the additive values of single cells but that the mass transfer behaviour of the stack did not exactly follow that of the single cell. The large number of cells (30) led to uneven heating, and the excess interior heat could not be easily dissipated. This resulted in a temperature gradient from the central interior of the stack to its exterior, with total temperature difference of up to 26 °C. Similarly, Bonnet et al. [32] found that at the same current density, a single cell and 5-cell stack both displayed voltage increases as cathode relative humidity increased from 10% to 60% under driving cycle tests; however, discrepancies appeared when the air relative humidity increased beyond 60%. The single cell voltage continued to increase with relative humidity, whereas the stack voltage decreased at humidities above 60%. They attributed this transition to the accumulation of liquid water at the anode.

In addition to comparisons between single cells and stacks, several authors [30,31,35,36] have compared stacks of different sizes to investigate the correlation between the number of cells and performance. San Martin et al. [35] compared the performance of two PEMFC stacks: a 10-cell, 40 W stack and a 47-cell, 1 kW stack. They observed a reasonable scaling effect for hydrogen flow rate, stack voltage, stack resistance, electrical power, and electrical efficiency. They also found that scaling provided a good prediction of fuel cell stack performance. However, auxiliary power demands did not meet the similarity criteria, since the 1 kW stack employed both a cooling fan and air compressor, while the 40 W stack only used a fan.

In some studies [30,31,36,37], it has been found that additional cells resulted in decreased stack performance. Notably, Fronk et al. [37] reported that stack reliability decreases and probability of failure increases when the number of cells (and stack voltage) increases. Dhathathreyan et al. [30] reported an overall reduction in stack performance when the number of cells increased from 24 to 50. They attributed this performance decrease to the increase in pressure drop and decrease in flow distribution associated with the larger stack. Giddey et al. [31] assembled stacks in 2-, 4-, 8-, and 15-cell configurations. In the largest stack, a temperature variation of up to 25 °C was measured across the stack due to uneven cooling. The 2- and 4-cell stacks exhibited the lowest ohmic resistance values. Their results indicate that additional cells may not be beneficial to stack performance, and that the reduction of contact resistance between cell components is necessary to reduce stack ohmic resistance.

2.2. Individual cell voltage uniformity

A common diagnostic tool in stack testing is the measurement of individual cell voltages within a stack in order to determine their variations along the stack [25,45–47,51–55,171,172]. Cell voltages have been shown to vary throughout the stack, and these measured discrepancies can be used as a tool to detect failed cells. This voltage non-uniformity has been shown to vary with stack operating conditions.

Cell voltages lower than the stack average have been detected in cells furthest from the fuel inlet of the stack (nearest to the air inlet) in dead-ended anode operation [25,51,54] as well as in non-dead-ended stacks [46,53] due to uneven gas distribution, water flooding, or low reaction temperatures. Cells furthest from the hydrogen inlet have exhibited the lowest voltage, as reported in [46,53]. In contrast, central cells have also been found to exhibit the lowest voltages [38–40,47]. This was attributed to membrane drying due to the high temperatures of the centre cells and uneven distribution of air flow between the cells [47].

Zhu et al. [25] investigated the uniformity of cell voltages within the 47-cell, 1 kW Ballard Nexa stack, and they found an average 8.8% deviation in cell voltage from the mean value. Similarly, Wang et al. [44] measured a 7% average deviation from the mean cell voltage in their 5 kW stack at open-circuit voltage. Uniformity was also measured at higher loads: a 5% voltage deviation was found by Rodatz et al. [28] at a current density of 0.34 A cm^{-2} in a 100-cell, 6 kW stack, and a 16% voltage deviation was found by Giddey et al. [31] under full load (0.53 A cm^{-2}) in their 15-cell, 1 kW stack. Zhu et al. [25] estimated that by increasing the average cell voltage with higher catalyst loading for the lower performing electrodes or by improving the gas distribution and purge system design, their stack power could be increased by 11.3%.

Non-uniformities in single cell potential along a stack are also indicators of localized defects. Rodatz et al. [28] recognised that monitoring stack voltage did not allow them to distinguish between the slight deterioration in all cells and the failure of a single cell. They observed that the failure of a single cell in a 100-cell stack reduced the stack voltage by only 1%, an amount that could also be attributed to membrane dehydration or electrode flooding throughout the stack. Therefore, they suggested monitoring every cell voltage in order to detect the failure of a single cell. Cell voltage drops can be early signals of hydrogen crossover or holes in the membrane [56]. By measuring individual cell voltages, Hinaje et al. [57] were able to detect a defective cell, which exhibited a voltage 100 mV lower than the other cells. However, single cell voltage drops indicate only the location and not the type of failure, such as flooding, overheating, or membrane failure [28]. Tian et al. [48] also proposed a method for detecting a failed cell, which involved monitoring cell open-circuit potentials after the removal of hydrogen flow. At open-circuit voltage, the failed cells displayed a rapid voltage loss, as a result of hydrogen crossover. This method was employed by Tian et al. in [48,58] to detect induced leaks in cells within various stacks.

The non-uniformity observed in cell voltages also varies with operating conditions. Voltage deviation has been shown to increase with increases in current density [31,41,45,49,54]. Fig. 3 by Ahn et al. [45] illustrates the voltage variation produced from their 40-cell, 2.89 kW stack, where the first cell is closest to the cathode air inlet. This increased deviation with current density was attributed to high rates of water production, which led to flooding [41]. Moçotéguy et al. [50,51] and Eckl et al. [38] found that the cell voltage distribution became increasingly less uniform with

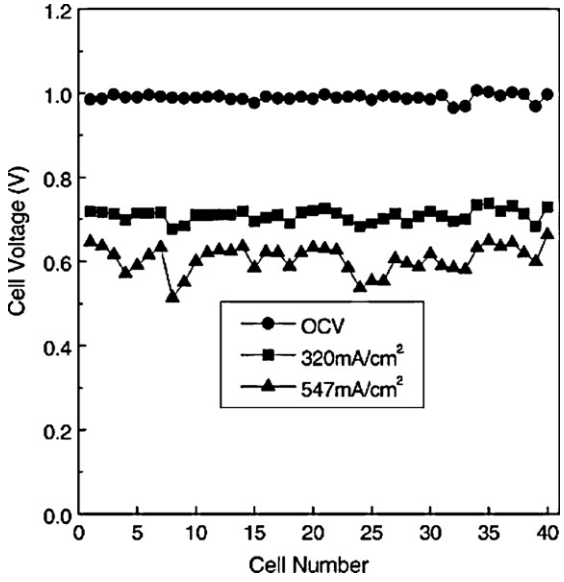

Fig. 3. Distribution of individual cell voltages within the 2.89 kW stack, reported by Ahn et al. [45].
Reprinted from [45] with permission from Elsevier.

the aging process. They attributed this to uneven dehydration [38] and the increased sensitivity of cell voltage uniformity to reactant utilization with aging [50]. In the work of Morner and Klein [59], cell voltage variation in their 22-cell stack was ±0.6 V at current densities above 0.08 A cm^{-2}, compared to ±0.2 V at current densities below 0.08 A cm^{-2}. Jang et al. [39] found that voltage deviation decreased with increasing fuel humidity, which they ascribed to the internal cell resistance drop, particularly in the centre cell. Perez-Page and Perez-Herranz [41] observed a more uniform cell voltage distribution at 70 °C compared to 40 °C, which they attributed to the increase in membrane conductivity with increased temperature. Squadrito et al. [43] found that cell voltage uniformity improved when the air flow rate increased from 8.7 L min^{-1} to 10.4 L min^{-1} in their 10-cell stack. They ascribed the remaining non-uniformity to uneven gas distribution in the stack.

In addition to cell voltage non-uniformity, distributions of temperature within a stack have also been recorded. Central cells in a stack have been found to have the highest temperatures [53]. Adzakpa et al. [27] measured variations of up to 8 °C from one cell to another. The temperature distribution within the stack was found to become more uneven at high current densities (above 0.4 A cm^{-2}), leading to higher cell temperatures in the centre than at the ends [47]. Such temperature variations lead to voltage differences between cells and reduced total stack power [27].

Rodatz et al. [28] attributed variations in cell voltages to several factors, including uneven flow distributions of reactant gases, non-uniform stack temperatures, varying aging states of cells, and cell defects. Non-uniform flow and temperature distributions directly affect water management, making a proper water balance more difficult to achieve in a stack than in a single cell [38]. Furthermore, the cell with the lowest voltage may limit the stack's maximum power output [28,42]. A robust control system is important to ensure stable and efficient operation, protect the stack from damaging operating conditions, and facilitate maximum stack lifetime. A stack control system should include individual cell voltage monitoring, though cost and wiring complexity should be accounted for in the design [56].

A patented technique has been proposed to mitigate stack temperature distributions by adjusting coolant flow during load changes [60]. Also, several patents suggest methods to improve the delivery of reactants through the use of one or multiple blowers [61], an inlet fuel gas distributor [62], and a flow field with central hole and flow grooves for uniform diffusion [63]. It has been suggested that more uniform operating conditions could also be achieved through the use of dual endplate humidifiers [64] and through system monitoring [65].

2.3. Influence of operating conditions on performance

The impact of system operating conditions on PEMFC stack performance has been a topic of popular interest [24,29,32,38–44,66–71,73–81]. System operating conditions include ambient temperature and relative humidity, cell temperature, reactant humidification, and reactant flow rate/stoichiometry.

2.3.1. Stack temperature

Stack power has been found to increase with increasing ambient temperature [24,76,77,81] and stack temperature [38,39,41,66,70,80] due to increased electrode reaction rate [76], mass transfer rate [38,80], gas diffusivity [41], and membrane conductivity [76]. In [76], Chu and Jiang found that stack power was lowest at an ambient temperature of 5 °C and increased with temperature up to 35 °C, and this trend was most visible at current densities above 0.1 A cm^{-2}. They attributed this trend to increases in reaction rate and ionic conductivity of the membrane at higher temperatures. In [24], the authors achieved more effective self-humidification of reactants and more effective mass transport at 30 °C compared to temperatures at 10 °C or lower. However, too large an increase in temperature caused thermal management problems and membrane dry-out, which led to reduced conductivity and high activation losses [24]. Dehydration was also observed at stack temperatures above 50 °C in [38,41].

2.3.2. Humidity

Cathode air humidity has also been shown to influence stack power, with increased performance at higher humidity levels [39,70,76,77] as a result of increased proton conductivity [76]. In [76], the highest power output occurred at 85% relative humidity for all current densities, and power decreased as humidity was lowered down to 20%. Below 20% relative humidity, the stack could only reach 5% of maximum stack power.

Improved performance has been observed with higher hydrogen relative humidity (up to 100%) [29,39,78] especially when low air humidities are employed [70]. The humidification of the anode helps counteract the effect of membrane dehydration at low air humidity and high current density [70]. Increased humidification at the anode resulted in the reduction of carbon monoxide (CO) poisoning [71] due to the increased reaction site surface area, which enabled the membrane to resist CO poisoning. Increased inlet gas humidification has also been shown to offset membrane failure, as a result of the reduced fluorine release rate [103]. Conversely, Jung et al. [77] found that at current densities above 0.25 A cm^{-2}, an increase in hydrogen humidification led to water flooding and stack power degradation. Overall, a balance in the proper humidification must be found, as too high of humidity levels may lead to flooding [38] due to the accumulation of liquid water and diffusive flux of liquid water to the anode [32].

2.3.3. Hydrogen flow rate and pressure

Chen and Zhou [107] and Bonnet et al. [32] did not observe any influence of hydrogen flow rate variation on cell voltages in their PEMFC stacks, and Bonnet et al. [32] found that high hydrogen flow rates enhanced the diffusive transport of water through the membrane from the cathode to anode. Additionally, a positive correlation between stack performance and hydrogen pressure has been shown in [44,79], wherein small pressure increases resulted

Table 1
Summary of optimal operating conditions for various PEMFC stacks.

Stack description	Optimisation criteria	Load (A)	Optimal conditions				Ref.
			Stack temp. (°C)	Relative humidity (%)	Gas pressure (MPa)	Stoichiometry	
30-Cell, 220 W	Electrical efficiency	10	40	100	0.01	Cathode 2.25	[74]
		15	40	75	0.02	Cathode 2.0	
		20	40	50	0.01	Cathode 1.68	
20 kW	Stack potential	–	–	–	–	Cathode 2–2.5	[83]
300 W	Stack potential	<12	40–50	–	–	–	[38]
		>20	55–60	–	–	–	
5 kW	Stack potential	–	70	–	–	–	[73]
5-Cell	Stack potential stability	–	–	70	–	–	[29]
5 kW	Stack potential	–	70	–	0.2	–	[44]
100 W	Stack potential	–	–	–	–	Cathode 3.5 Anode 1.5	[67]
100 W	Stack potential	–	–	–	–	Cathode 5 Anode 2	[68]
20-Cell, 2 kW	Stack potential	–	–	60–80	–	Cathode 2.5–3	[69]

in measurable increased stack voltages. In [44], at 0.4 A cm^{-2}, an increase from 1 bar to 2 bar resulted in a 1 V stack voltage increase.

2.3.4. Optimisation

PEM stack performance optimisation involves a number of trade-offs. For example, improved lifetime may be sacrificed when reducing the overall cost or improving the power density [72]. Hydrogen quality must be balanced with stack durability, auxiliary power for start-up balanced with start-up time, and the rated power balanced with electrical efficiency [1]. With respect to specific operating parameters, the choice of stoichiometric ratio requires a trade-off between greater reactant flux and better performance with increased fuel costs [82]. Regarding water management, a delicate balance must be found between flooding and dehydration [67,83]. With respect to stack temperature, a balance between heat production and heat dissipation must be found in determining the appropriate operating temperature [22]. As the stack performance depends greatly on the operating parameters, several authors [29,38,42–44,67–69,73–75] have attempted to determine the optimal conditions for performance. Table 1 summarizes the proposed operating conditions for optimal stack potential or electrical efficiency, according to reported experimental test results.

Adegnon et al. [74] showed that optimal electrical efficiency can be achieved through the selection of parameters including stack temperature, air relative humidity, stoichiometric ratio, and reactant pressure. Depending on the load current, an optimal set of parameters was proposed. For example, at 10 A the highest electrical efficiency was found at 40 °C, 100% relative humidity, 2.25 air stoichiometric ratio, and 10 kPa. Eckl et al. [38] reported an optimal temperature of 60 °C for a 300 W stack (at load currents above 12 A), while 70 °C was proposed by Laurencelle et al. [73] and Wang et al. [44] for 5 kW stacks. These results may suggest that larger stacks have higher ideal operating temperatures, but this correlation has not been experimentally determined or mentioned in literature.

Similar to the proposal of optimal air (cathode) stoichiometry by Adegnon et al. [74], Corbo et al. [83] determined that an air stoichiometry of 2–2.5 led to optimal stack performance, especially at higher loads, while Yan et al. [69] suggested a value between 2.5 and 3. In their optimisation of stack operating conditions through experimental design and the use of Matlab's optimisation toolbox function, Wahdame et al. [67,68] determined that a stoichiometry of 1.5–2 for the anode and 3.5–5 for the cathode led to the highest stack voltage and performance.

Corbo et al. [75] identified a region of optimal operation of a PEMFC stack with respect to the stack power and temperature, which was verified in tests under European driving cycles with a 6-cell, 2.4 kW stack. Fig. 4 highlights the region of preferred operating power and temperature, indicating that operating points in regions A and B lead to flooding and drying out, respectively. When operating within region A, the purge frequency must be increased and heat removal decreased. If the working point is within region B, the stack temperature must be increased and more water injected.

Philipps et al. [42] varied the air stoichiometric ratio at several different current steps to determine the relationship between air pressure and system power, determining optimal parameters for each load setting to maximise the output power. Optimal air pressure increased with increasing current. They found that an air pressure of 1.8 bar was required to achieve maximum power at 120 A for their 120-cell, 11.5 kW stack.

2.4. Electrochemical methods for studying stack performance

A commonly employed technique for quantifying PEMFC performance is through the polarization curve, which provides information regarding performance losses including activation, ohmic, and mass transport, and allows the comparison of performance in various operating conditions. The limitation of polarization curves is that they do not provide information about individual stack components, and cannot differentiate loss mechanisms such as dehydration or flooding. In addition to the polarization curve, there are several electrochemical methods employed in PEMFC stack testing, which are described below.

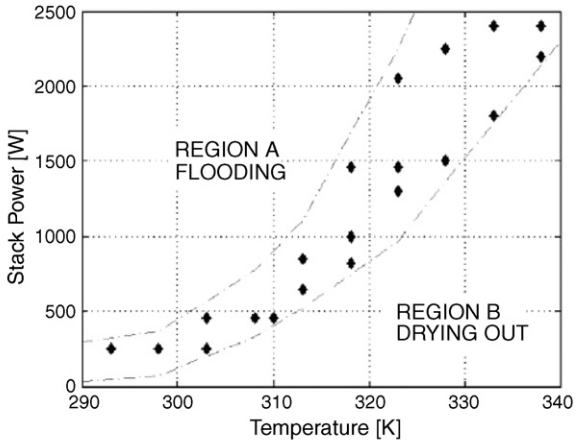

Fig. 4. Correlation between stack power and temperature for determining the optimal operating region for a 2.4 kW stack, reported by Corbo et al. [75].
Reprinted from [75] with permission from The International Journal of Hydrogen Energy.

2.4.1. Current interrupt

Another analytical electrochemical technique is the current interrupt (CI) method, wherein current is removed from the stack periodically to measure the transient voltage response to load changes. Ohmic losses can be determined from the difference in voltage immediately before and after the current removal [20]. Because the ohmic losses in a stack disappear more quickly than activation losses, it is possible to distinguish between the two types of losses, unlike in a polarization curve. Another advantage of the CI method is the ease of data analysis [89]. However, without rapid data collection it is difficult to determine the exact point of voltage rise [89]. CI has been used in several stack investigations, to measure stack resistance [33,34,40], measure individual cell ohmic resistance [47], isolate poorly performing cells [47], and measure the stack ohmic losses at various temperatures [84]. CI has also been used to maintain isothermal stack temperatures in order to compare performance at various temperatures [25,35].

2.4.2. Cyclic voltammetry

Cyclic voltammetry (CV) is a method used to investigate catalyst activity. In the CV method, the working electrode is flushed with nitrogen and the other electrode flushed with hydrogen. Using a potentiostat, the system potential is swept between two voltage limits while current is recorded, and a plot of current vs. voltage (voltammogram) is created [89]. The electrochemical surface area (ECSA) is then determined from the detected hydrogen adsorption and desorption activity [12]. A disadvantage of this technique is the masking of hydrogen adsorption and desorption by carbon, which can be avoided through low voltage sweep limits [89]. CV has been employed in several stack-level tests to measure the ECSA [30,46], and to study membrane degradation by determining the loss of ECSA during operation [45,85–87,90].

2.4.3. CO stripping voltammetry

In CO stripping voltammetry, carbon monoxide (CO) and inert gas are fed to one electrode, while hydrogen is fed to the other. Then, pure argon is fed to the active electrode to remove any CO, and the potential is then swept (in a method similar to CV) to record a CO stripping voltammogram (plot of current density vs. potential) and to measure the ECSA [89]. However, CO stripping voltammetry is more commonly employed at the single cell level than stack-level.

2.4.4. Linear sweep voltammetry

Linear sweep voltammetry (LSV) is an electrochemical method employed to measure hydrogen crossover through the membrane [48]. As in CV, hydrogen and nitrogen are fed to the anode and cathode, respectively, and the potential is swept between two limits in only one direction (linearly instead of cyclically). Electrochemical activity in the form of current is monitored to determine the current density at which hydrogen oxidation occurs [86]. LSV has been employed in few stack-level investigations [86,88], limited mostly to single cell testing. The most common electrochemical method used in stack testing is EIS, as described below.

2.4.5. Electrochemical impedance spectroscopy

To obtain a more in-depth analysis of stack performance, the technique of electrochemical impedance spectroscopy (EIS, or ac impedance) can be employed to study both steady-state and dynamic behaviour. In EIS, ac perturbation signals are applied to a system to measure the system's ability to impede electrical current. Using a frequency response analyser, the resulting current or voltage signals are measured to determine the different types of losses: ohmic, kinetic, and mass transport. The advantage offered by EIS analysis over polarization curves is that the individual contributions of each type of loss can be determined within a short period of time [89]. Yuan et al. [91] provided a comprehensive overview of ac impedance measurement techniques for characterizing PEMFC performance, citing both single cell and stack testing. The applications of EIS in PEMFC research included optimisation of the MEA structure, understanding of contamination, stack and cell impedance, localized impedance [91], and insight into MEA aging [68].

EIS has been employed to characterize water management in a fuel cell stack, especially for detecting and distinguishing between flooding and dehydration [20,92–94]. Le Canut et al. [94] employed EIS to detect and distinguish between membrane drying, fuel cell flooding, and carbon monoxide poisoning based on the impedance response. Flooding was detected via large impedance magnitudes and large voltage oscillations. Hakenjos et al. [93] used the technique to observe flooding, and with EIS, flooding was detectable minutes earlier than it could be detected from observations of a voltage drop in a polarization curve. Ciureanu [92] studied the dependence of ohmic resistance on current under varying humidification conditions. They detected dehydration and proposed that a decrease in the active electrocatalyst surface area led to cathode deactivation, and thus, cathode dehydration.

EIS can be employed to detect both stack impedance and the impedance of each cell, by measuring individual cell impedances. Several authors [26,66,93,95,173] found good agreement between the sum of single cell impedances and the overall stack impedance. Using a 4-cell, 10 W stack, Diard et al. [96] were among the first groups to determine single cell impedance, which they calculated separately for each cell from impedance measurements of both the load (a power resistor) and the load and stack (in parallel). In a two-part investigation, Yuan et al. [26,80] performed an ac impedance diagnosis of a 6-cell, 500 W stack and studied both stack and individual cell impedance. They found good agreement between the total stack ohmic loss and the sum of individual cell ohmic losses. Andreasen et al. [66] utilized EIS to develop a model of a high-temperature PEMFC stack, basing it on the fact that stack impedance resembles that of an individual cell in the stack. They found that individual cell impedances could be used to predict stack impedance, which is beneficial since auxiliary electronic components may introduce measurement interference at a stack-level. Zhu et al. [95] found that the activation loss for groups of cells was approximately equal to the sum of single cell activation losses. Hakenjos et al. [93] measured the impedance of all four single cells in their custom-made stack simultaneously, and found that the sum of the single cell impedances was within 2.5% of the whole stack impedance.

As is seen with cell voltage, impedance may be non-uniform throughout a stack. Yuan et al. [26] found that their stack's centre cells exhibited lower ohmic resistances due to higher local temperatures. Diard et al. [96] found that impedance was highest at the cell furthest from the gas inlet. They attributed this to gas starvation as the fuel moved through the stack, and they suggested a stack design with different cell active areas to compensate for this impedance non-uniformity.

Fuel cell operating conditions have an impact on the stack impedance. Yan et al. [69] investigated the ac impedance characteristics of a 20-cell, 2 kW PEMFC stack under varying operating conditions, showing that air stoichiometry significantly affected the stack's impedance. Mass transfer resistance decreased from approximately 18 $\Omega\,cm^{-2}$ to 3 $\Omega\,cm^{-2}$ by increasing air stoichiometry from 1.5 to 4. They attributed this to an increased oxygen concentration of reactant gas in the stack and more effective water removal from the cathode at higher air stoichiometries. Air humidity and operation temperature influenced the mass transport loss to a lesser degree, decreasing by only 1 $\Omega\,cm^{-2}$ with a temperature increase from 30 °C to 60 °C and by 3 $\Omega\,cm^{-2}$ with an increase in relative humidity from 20% to 60%. Both stack impedance and ohmic losses decreased as relative humidity increased from 20% to 80%,

Table 2
Summary of achieved PEMFC stack durability.

Stack description	Test length (h)	Voltage decay	Causes of performance loss or failure	Ref.
40-Cell, 2.89 kW	1800	–	a, b	[45]
5-Cell, 600 W	550	8%	–	[32]
10-Cell	7863	11 $\mu V\,h^{-1}$	–	[97]
9-Cell	1000	5–10 $\mu V\,h^{-1}$	–	[30]
40-Cell, 5 kW	1000	40 $\mu V\,h^{-1}$	–	[104]
15-Cell	2000	20 $\mu V\,h^{-1}$	c	[85]
15-Cell	2000	25 $\mu V\,h^{-1}$	c	
60-Cell, 10 kW	400	–	d	[49]
2-Cell	2000+	10 $\mu V\,h^{-1}$	–	[71]
8-Cell	3000	–	e	[72]
10-Cell	1100	–	None	
17-Cell	13,000	0.5 $\mu V\,h^{-1}$	–	
64-Cell, 1 kW	500	27 $\mu V\,h^{-1}$	–	[105]
32-Cell	3239, 3836	10 $\mu V\,h^{-1}$	e	[100]
36-Cell	668	17–36 $\mu V\,h^{-1}$	–	[98]
80-Cell, 5 kW	640	72.5 $\mu V\,h^{-1}$	–	[84]
10-Cell	200	–	a	[87]
24-Cell, 500 W HT-PEMFC	658	200–520 $\mu V\,h^{-1}$	–	[50]
24-Cell 500 W HT-PEMFC	658	7.6%	–	[51]
100-Cell	500	–	f, g	[46]
1 kW (Unit A)	1875	–	e at 800 h, h at 1178 h	[101]
1 kW stack (Unit B)	1653	–	e at 1460 h, no h	
3-Cell	800	60 $\mu V\,h^{-1}$	d	[52]
50-Cell	2500	20 $\mu V\,h^{-1}$	–	
8-Cell	5800	1 $\mu V\,h^{-1}$	–	[19]
8-Cell, 20 kW	11,000	2 $\mu V\,h^{-1}$	–	[102]
3-Cell, 100 kW	1000	10 $mV\,h^{-1}$ after 350 h, 0.22 $mV\,h^{-1}$ after 400 h	–	[67]
3-Cell, 100 kW	700	1 $mV\,h^{-1}$ in first 500 h	–	
3-Cell	1000	–	h at 450 h	[68]
6-Cell	1200	0.128 $mV\,h^{-1}$	a, then h at 800 h	[86]
20-Cell, 0.4 kW	5000	1.5 $\mu V\,h^{-1}$	–	[106]
4-Cell	1000	0.18–0.26 $mV\,h^{-1}$ thinner membranes 0.09 $mV\,h^{-1}$ thicker membranes	a, e	[88]

a – catalyst degradation.
b – MEA contamination.
c – Pt surface area loss.
d – insufficient water removal.
e – crossover leak.
f – increased internal resistance.
g – decreased active area.
h – membrane or cell failure.

due to improved membrane conductivity. Values of ohmic, charge, and mass transfer resistances all gradually decreased as operating temperature increased from 30 °C to 60 °C. Yan et al. [69] also performed ac impedance analysis under load changes and found that the membrane water content gradually decreased at low loads, but increased at high loads. Therefore, to balance the water content, it was necessary to adjust the reactant gas humidity as the load varied. Yan et al. [70] measured membrane resistance via ac impedance at various humidity levels. They observed increased membrane resistance with decreases in relative humidity of the feed gas, as well as increased internal resistance with decreases in air inlet relative humidity. In addition to determining the stack impedance, by monitoring the impedance of individual cells within a stack, it is possible to detect a failure that occurs in a single cell [96].

2.5. Lifetime/endurance testing and degradation

2.5.1. Lifetime/endurance testing

An important factor for fuel cell implementation is the lifetime (endurance) of the device. The US Department of Energy (DOE) has set targets of 20,000 h (as of 2005) to 40,000 h (as of 2011) for stationary applications and 5000 h for transportation applications [1].

Table 2 summarizes the endurance tests available in the literature, including degradation levels and other sources of performance losses. Though many lifetime tests have shown that voltage degradation may be relatively low, reports by Ballard Power systems [19,72,97,102] are among the few who have reported sufficiently long lifetimes. An example is the 13,000 h test by Knights et al. [72], shown in Fig. 5. This deficit in lifetime testing in the literature demonstrates the need for real-life endurance testing with stack systems, particularly for demonstrations, examples of which are listed in Section 2.7.

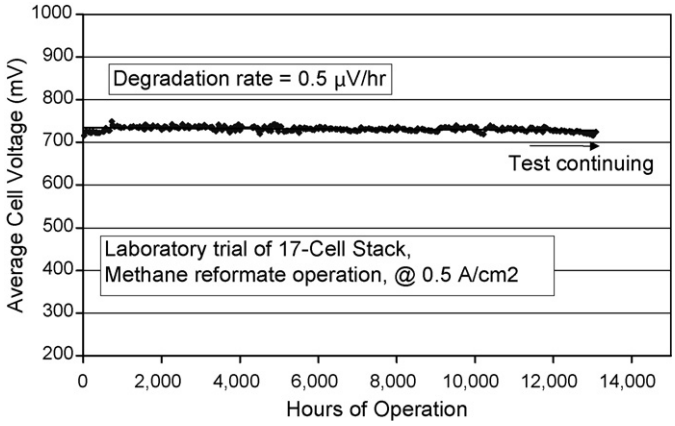

Fig. 5. Endurance test of a 17-cell stack comprised of 250 kW natural gas power plant hardware, reaching over 13,000 h operation, reported by Knights et al. [72]. Reprinted from [72] with permission from Elsevier.

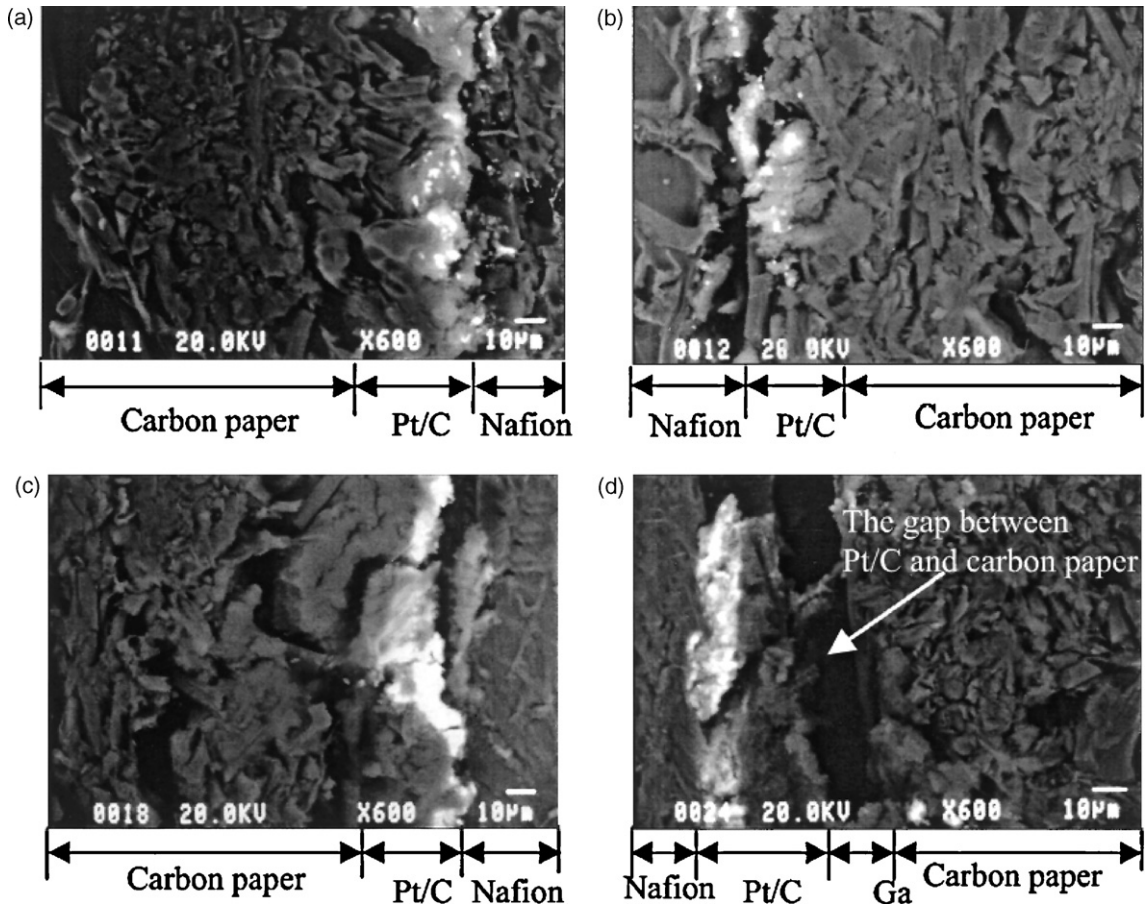

Fig. 6. Images of MEA before and after 1800 h of operation (a) anode before, (b) cathode before, (c) anode after, (d) cathode after, as reported by Ahn et al. [45]. Reprinted from [45] with permission from Elsevier.

In addition to cell voltage decay, the performance losses during lifetime tests are caused by reduced activation area [46], increased internal resistance [46], hydrogen leaks [101] leading to membrane failure [68,72], catalyst decay [45,87], and membrane contamination [45].

2.5.2. Degradation in PEMFC stacks

Stack-level degradation has been investigated in several studies [45,46,50,51,57,87,88,90,99,103,108,174]. Test results have shown a reduction in active surface area, increased internal resistance, membrane thinning, holes or leaks in the membranes, electrode destruction, and reduced adhesion of electrodes to membranes [57]. However, additional studies are necessary to determine any differences between the degradation of stacks and single cells.

Performance degradation has been shown to be uneven throughout the stack by Pei et al. [46], who investigated the degradation of a PEMFC stack after a 500-h accelerated lifetime test. They found that the catalysts in the hydrogen inlet region remained active, in contrast to the low activity of catalysts in other sections. The ECSA was greatly reduced, but a larger loss in surface area was noted in certain cells than in others. The stack internal resistance doubled, and the average catalyst particle diameter tripled. They attributed these behaviours to non-uniform gas intake and water distribution. Moçotéguy et al. [50,51] also found uneven performance degradation in both steady-state and dynamic tests with their 24-cell stack.

Additionally, it has been shown that degradation rate is dependent on initial membrane thickness. Yuan et al. [88] tested a 4-cell stack for 1000 h under idle conditions to measure the membrane degradation of each cell. Though the thinner membranes performed favourably before the test, the thinner membranes displayed more rapid rates of degradation than thicker. This degradation was caused by hydrogen crossover, which indicated membrane thinning and hole formation. Li et al. [103] showed that membrane thickness decreased with time during a steady-state test of a 5-cell stack. They attributed this thickness decrease to the degradation of the cathode ionomer, which was almost completely corroded after 130 h.

Ahn et al. [45] investigated the causes of degradation in their 40-cell stack through various electrochemical methods. After 1800 h continuous operation, they found silicon at the catalyst layer, and oxygen in the form of platinum oxide at the cathode. These findings indicated that catalyst degradation and MEA contamination led to stack failure. As shown in Fig. 6, the catalyst layer is separated from the carbon paper at the cathode side due to mechanical stress.

The decay of the Pt/C catalyst has been found to be greater than that of the polymer membrane by Luo et al. [87], who investigated the degradation of a 10-cell stack as a result of 200 h of testing. As shown in Fig. 7, the Pt particles displayed aggregation without crystal lattice change. The study also showed that the oxygen reduction potential of the catalyst reduced from 0.48 V to 0.4 V. Degradation was also attributed by Zhang et al. [99] to Pt catalyst agglomeration during freeze/thaw cycles.

As there have been limited stack-level studies focused on the degradation, the reader is referred to review papers [10,12,13,20] that address PEMFC degradation issues in-depth at the single cell level. Despite their discussion of degradation in single cells rather than in stacks, these reviews summarize the main aspects of PEMFC degradation, and the contributions of single cell tests are valuable

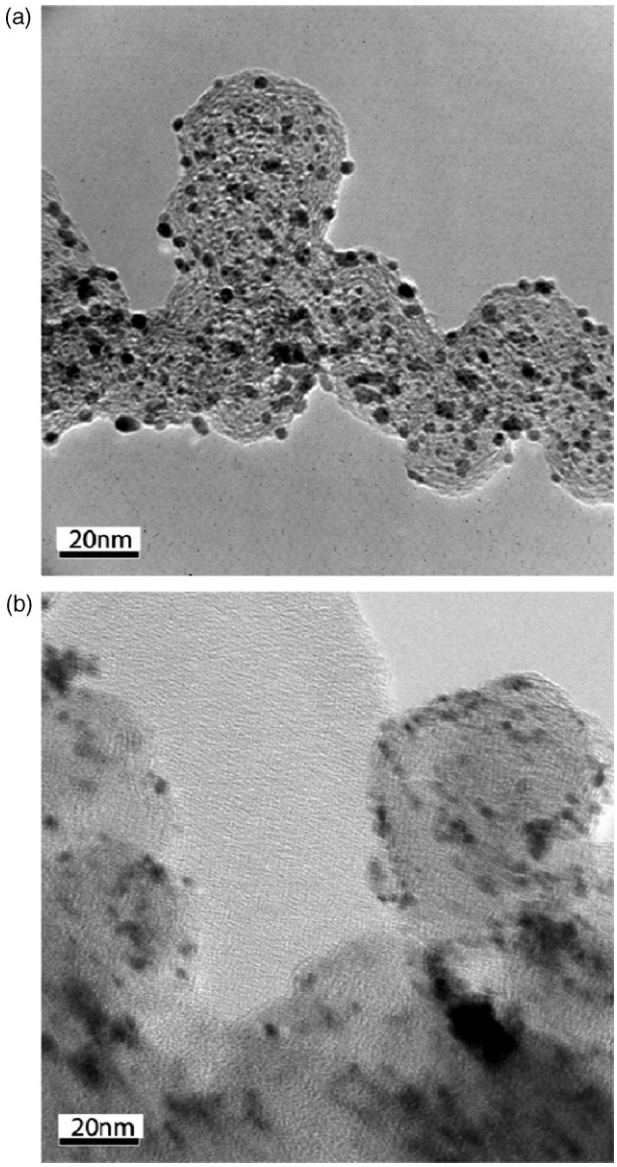

Fig. 7. Comparison of Pt/C catalyst of 4-cell stack (a) before and (b) after 200 h steady-state testing, reported by Luo et al. [87].
Reprinted from [87] with permission from The International Journal of Hydrogen Energy.

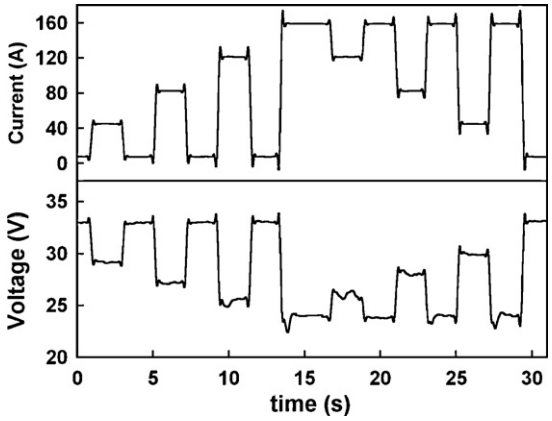

Fig. 8. Demonstration of stack current and voltage response to load variations as a function of time for a 35-cell, 5 kW PEMFC stack, reported by Hamelin et al. [113].
Reprinted from [113] with permission from The International Journal of Hydrogen Energy.

to stack research in this aspect. Knights et al. [72] reported that a degradation rate of 2–10 $\mu V\,h^{-1}$ is common for most applications. However, stack degradation, especially the differences between degradation in single cells and in stacks, should be investigated further.

2.6. Dynamic testing

Transient behaviour, such as frequent load changes and start–stop cycles, is highly likely to occur in commercial applications of PEMFC stacks, especially in non-stationary applications, such as transportation. It has been found that prolonged dynamic loading may shorten stack lifetimes, and the longer a stack operates in transient conditions, the more corrosion and deterioration will occur [109]. Comprehension of the dynamic response to load changes is important for optimal and reliable performance [110]. For these reasons, several studies have been performed to better understand stack response to transient changes. While many studies aim to identify dynamic stack behaviour and characterize the transient response of a PEMFC stack [14,70,73,107,111–119], some studies additionally aim to simulate the actual load changes experienced in specific applications [32,42,46,67,84,97,120,121], such as drive cycles in buses or cars. These commercial applications also include cold (sub-zero) start-ups [1,31,99,108,109,122–131] and start-up and shutdown cycles [10,31,46,51,98,132] as other forms of dynamic stack testing.

2.6.1. Dynamic response

The dynamic response of a PEMFC stack has been investigated by several authors [73,112–115]. Schiavetti and Del Prete [114] measured the dynamic response of a self-humidifying, air-breathing stack by varying the power between 120 W and 170 W to simulate an urban drive cycle. They reported an average response time of 0.033 s, and observed that the PEMFC responded quickly enough to be used in vehicle applications on the road. Stack behaviour under load variations approximately every 2 s was investigated by Hamelin et al. [113] (see Fig. 8), where the stack current and voltage response was faster than 0.15 s. However, as seen in Fig. 8, current and voltage transients (overshoots and undershoots) were observed and found to dissipate in less than 0.025 s. These transients were proportional to the size of the load current steps; the largest overshoots occurred with large current steps of more than 100 A. The same stack was used in [73] to test rapid load variations, where current transient dissipation took less than 1 μs. However, they found that the voltage reaction time was slower (approximately 1 s). The voltage exhibited undershoot behaviour, first dropping by up to 2 V below the polarization curve before stabilizing to its expected value. The dynamic response of an 8-cell stack to current steps was investigated by Yan et al. [70], who found that their stack response to load variations was similar to that in tests with a single cell. Unlike in the single cell tests, however, they observed voltage transients that corresponded to the size of the current step.

2.6.2. Flow management

Wahdame et al. [67] found that flow management strategies impacted stack durability during dynamic operation, such as mechanical stress resulting from pressure drops and hot spots appearing due to uneven reactant/product flow in cells. Corbo et al. [121] also investigated flow management in dynamic operation. In their study, a 20 kW stack was tested under cycles similar to those

found in automotive applications. They focused on the impact of the air management strategy, and found that excess cathode air (slightly higher than the optimal amount for stationary conditions) led to improved stack performance and cell voltage uniformity under dynamic conditions.

2.6.3. Flooding

During dynamic operation, pressure drops can indicate the presence of liquid water [107,175]. Chen and Zhou [107] investigated the dynamic responses of a 10-cell stack during start-up and after current step-ups. During both testing scenarios, they found that stack voltage oscillated due to flooding and recovery cycles, and that stack voltage could be correlated with the frequency of cathode and anode pressure drops. The dominant frequency of the cathode pressure drop signal was found to indicate the onset of flooding, which preceded a voltage drop. They suggested that cathode pressure drop signal frequency could function as a useful PEMFC diagnostic tool for flooding. Pei et al. [175] also suggested that measuring the hydrogen pressure drop is useful for predicting liquid water flooding in stacks.

2.6.4. Cold starts

Stack start-up in sub-zero temperatures must be possible for several practical applications, such as outdoor stationary or transportation in cold winter climates. Cold starts present several technical challenges. For example, frozen residual water in the stack may impede cold start-ups [122]. Additionally, product water may freeze immediately during operation, blocking catalyst and gas diffusion layer pores, or blocking flow paths [99,109,122]. The US Department of Energy has set a requirements of achieving rated power at −20 °C in less than 30 s from a cold start by 2011 [1]. Common types of cold start investigations include achieving the shortest possible start-up time, determining lowest acceptable temperature for cold start, and measuring performance degradation due to cold starts [31,108,123–131].

Regarding acceptable cold start temperatures, Oszcipok et al. [123] successfully started a 6-cell stack at −10 °C. By increasing the start-up load from 1 A to 2.8 A, the time to reach 0 °C stack temperature decreased from 17 min to 4 min. At −20 °C a successful cold start was not possible, as the stack temperature could not be brought above 0 °C through passive operation. Similarly, Schießwohl et al. [124] found that a successful cold start was possible at −10 °C with their 60-cell, 2.6 kW stack, with a maximum start-up time of 460 s. They reported that below −10 °C, an external heating device would be necessary.

Alink et al. [108] investigated the degradation effect of sub-zero operation at temperatures as low as −40 °C with two 6-cell stacks. In the stack that was dried before cooling, degradation was negligible. In contrast, the stack subjected to wet freezing displayed significant performance degradation, and higher load operation was no longer possible after several sub-zero exposures. This work demonstrated that the level of degradation was dependent on freezing conditions, and that water should be removed before freezing occurred, otherwise material changes would be caused by volume expansion at low temperatures.

Bégot et al. [125] studied the influence of operating parameters on the cold start of a 2 kW PEMFC stack, finding that low current density, high initial impedance, high gas flow rate, low gas pressure, and low coolant rate positively impacted cold start performance. In their study of the operating conditions and cold start-up, Oszcipok et al. [123] found that dry membranes and high air flow rates were beneficial to successful cold starts. They attributed this to higher water uptake by drier membranes, and better water removal at higher air flow rates.

Patented techniques have been developed for the improvement of cold starts of PEMFC stacks. Several patents propose more energy efficient cold start-ups through sub-zero temperature detection [126], auxiliary load (heater) [126,127], the removal of liquid water upon shutdown [128,129], delivery of dry reactants before shutdown and after start-up [130], and the melting of coolant water through an oxidant manifold [131].

2.6.5. Start/shutdown cycles

In addition to cold starts and dynamic operation, start-up and shutdown (start/stop) cycles can be employed to measure the durability of a stack, as a form of accelerated testing to mimic commercial operation, especially relevant for vehicles.

Start/stop cycles have been shown to cause additional degradation in the PEMFC. Hydrogen crossover occurs during shutdown, so that in the subsequent start-up, fuel starvation occurs at the outlet. Therefore, start/stop cycles can lead to significant damage; however the effect can be minimized through potential control (voltage clipping) [10,176]. During start/stop cycles, air leakage can result in a hydrogen/air front at the anode, and this can lead to cell voltages higher than 1.2 V, where carbon corrosion is accelerated [132].

Stack-level start/stop cycling has been employed to investigate the degradation effect of commercial stack operation [46,51,100]. Moçotéguy et al. [51] found that start/stop cycling caused a higher degradation rate than that found in steady-state operation. Start/stop cycles can also be carried out in sub-zero temperatures (see Section 2.6.4) in order to study the effect of freezing on cyclical start-up and shutdown behaviour, but only a few studies [31] have employed this method.

2.7. Stack demonstrations

Several demonstration projects have been conducted around the world [177], ranging from backup power [101,133–139] (especially in telecommunications [100,140–147]), automotive [148–159], to cogeneration in both residential [160–165] and hybrid systems [98,166–170]. The current status of fuel cell technology for mobile and stationary applications has been discussed in several reviews [178–181]. Examples of tests performed in the aforementioned literature include life tests, cold starts after idle periods, and overall performance under various loading and environmental conditions, but due to the proprietary nature and scarcity of published measurements, detailed performance of stack demonstrations is not yet well understood.

3. Conclusions and future opportunities

In this paper, we provided a review of PEMFC stack testing, with a discussion of the main topics of investigation, including single cell vs. stack-level performance, cell voltage uniformity, influence of operating conditions, durability and degradation, dynamic operation, and stack demonstrations.

Although polarization curves have been demonstrated to scale well from the single cell to stack-level, single cell performance alone cannot be employed to predict that of a stack due to the coupling of stack size with heat and mass transfer. Several studies have suggested that stack performance suffers as a result of increased number of cells in the stack, but there is still uncertainty regarding the degree of influence that the number of cells has on stack performance. Further performance comparisons of varying stack sizes are needed.

The impact of cell voltage uniformity on fuel cell performance requires further investigation. Furthermore, whether cell voltage uniformity should be based on open-circuit voltage or in operation should be determined. It would also be valuable to determine a range of cell voltage distributions that would be tolerable for commercial stack performance.

Although many studies of Section 2.3 suggest optimal operating conditions for best stack performance, there is a wide range of results concerning how operating conditions impact stack power and electrical efficiency. The operating conditions for best performance require a balance between temperature, humidity, and reactant flow rates to avoid both flooding and dehydration. The influence of operating conditions at stack vs. single cell level should be investigated further to determine if single cells and stacks exhibit differing sensitivities to operating parameters. Additionally, the influence of operating conditions for different stack sizes and number of cells requires investigation to determine whether conditions for best performance vary with stack dimensions.

There are several electrochemical methods available to investigate PEMFC behaviour. While polarization curves and CV are widely used for stacks, CO stripping and linear sweep voltammetry are still mostly limited to single cell research. In order to better understand membrane degradation and hydrogen crossover in stacks, these latter two techniques must be used more frequently in stack-level studies. The most common electrochemical method, EIS, is a useful technique to determine flooding locations and to understand aging within a stack, and the impedance of single cells scales well to predict stack-level impedance. The employment of EIS under various operating conditions can help to determine the best temperature, humidity, and flow rates required to achieve minimal performance losses and to achieve high efficiencies. We recommend that this technique should be more widely incorporated into stack-level testing to optimise stack-level operating conditions. Additionally, there is an opportunity to employ EIS techniques in field trials to determine the impact of commercial load cycles on stack impedance.

Stack degradation, especially the differences between durability of single cells and stacks should be investigated further. There is a need to understand the behavioural differences in stacks and individual cells and the effect of scaling on degradation. Degradation in commercial stacks should also be investigated, as this degradation is likely influenced by dynamic loads and variable environmental conditions.

Regarding dynamic operation, there is an opportunity for additional comparisons between degradation in steady-state and dynamic testing. Degradation has been shown to be greater with dynamic loading, but the difference has not been quantitatively verified. Additionally, the transient behaviour of a stack following load variations has been investigated, but further investigations are needed to determine the impact of transient responses on overall stack performance and durability. Though the technique of start/stop cycling is understood to escalate PEMFC degradation, additional start/stop cycling investigations are necessary to determine the effect at the stack level as compared to that which occurs in single cells. Insight into the nature of degradation caused by start/stop cycling would benefit from isolating the effects of other accelerated testing methods such as loading cycles and cold starts.

Additional endurance testing is required to meet lifetime requirements, and an opportunity exists to integrate endurance testing in field trials. Field trials have typically lacked controlled experimental conditions required for quantifiable results. The most frequently reported findings include successful start-up, overall availability (percentage of time a system is operational), and reliability (percentage of time a system performs as expected). It is recommended that future field trial investigations include quantitative results, so that commercial demonstrations can be compared to laboratory tests.

The recommendations for future work described above will also lead to much-needed empirical data for model validation that will benefit the development of predictive stack-level computational models.

Acknowledgements

The Bullitt Foundation and the University of Toronto are gratefully acknowledged for their financial support.

References

[1] Department of Energy, Technical Plan – Fuel Cells, Department of Energy, 2007.
[2] A. Faur Ghenciu, Curr. Opin. Solid State Mater. Sci. 6 (2002) 389–399.
[3] S. Litster, G. McLean, J. Power Sources 130 (2004) 61–76.
[4] V. Mehta, J.S. Cooper, J. Power Sources 114 (2003) 32–53.
[5] B. Smitha, S. Sridhar, A. Khan, J. Membr. Sci. 259 (2005) 10–26.
[6] B. Wang, J. Power Sources 152 (2005) 1–15.
[7] A. Hermann, T. Chaudhuri, P. Spagnol, Int. J. Hydrogen Energy 30 (2005) 1297–1302.
[8] X. Li, I. Sabir, Int. J. Hydrogen Energy 30 (2005) 359–371.
[9] H. Tawfik, Y. Hung, D. Mahajan, J. Power Sources 163 (2007) 755–767.
[10] R. Borup, J. Meyers, B. Pivovar, Y. Kim, R. Mukundan, N. Garland, et al., Chem. Rev. 107 (2007) 3904–3951.
[11] A. Collier, H. Wang, X. Zi Yuan, J. Zhang, D.P. Wilkinson, Int. J. Hydrogen Energy 31 (2006) 1838–1854.
[12] F. De Bruijn, V. Dam, G. Janssen, Fuel Cells 8 (2008) 3–22.
[13] J. Wu, X. Yuan, J. Martin, H. Wang, J. Zhang, J. Shen, et al., J. Power Sources 184 (2008) 104–119.
[14] S. Zhang, X. Yuan, H. Wang, W. Mérida, H. Zhu, J. Shen, et al., Int. J. Hydrogen Energy 34 (2009) 388–404.
[15] X. Cheng, Z. Shi, N. Glass, L. Zhang, J. Zhang, D. Song, et al., J. Power Sources 165 (2007) 739–756.
[16] A. Bazylak, Int. J. Hydrogen Energy 34 (2009) 3845–3857.
[17] M. Eikerling, J. Electrochem. Soc. 153 (2006) E58–E70.
[18] H. Li, Y. Tang, Z. Wang, Z. Shi, S. Wu, D. Song, et al., J. Power Sources 178 (2008) 103–117.
[19] J. St-Pierre, D. Wilkinson, S. Knights, M. Bos, J. New Mater. Electrochem. Syst. 3 (2000) 99–106.
[20] N. Yousfi-Steiner, P. Moçotéguy, D. Candusso, D. Hissel, A. Hernandez, A. Aslanides, J. Power Sources 183 (2008) 260–274.
[21] S.K. Das, A.S. Bansode, Heat Transfer Eng. 30 (2009) 691–719.
[22] S.G. Kandlikar, Z. Lu, Appl. Therm. Eng. 29 (2009) 1276–1280.
[23] J. Pharoah, O. Burheim, J. Power Sources 195 (2010) 5235–5245.
[24] D. Chu, R. Jiang, J. Power Sources 80 (1999) 226–234.
[25] W. Zhu, R. Payne, D. Cahela, B. Tatarchuk, J. Power Sources 128 (2004) 231–238.
[26] X. Yuan, J. Sun, H. Wang, J. Zhang, J. Power Sources 161 (2006) 929–937.
[27] K. Adzakpa, J. Ramousse, Y. Dubé, H. Akremi, K. Agbossou, M. Dostie, et al., J. Power Sources 179 (2008) 164–176.
[28] P. Rodatz, F. Büchi, C. Onder, L. Guzzella, J. Power Sources 128 (2004) 208–217.
[29] F. Urbani, O. Barbera, G. Giacoppo, G. Squadrito, E. Passalacqua, Int. J. Hydrogen Energy 33 (2008) 3137–3141.
[30] K. Dhathathreyan, P. Sridhar, G. Sasikumar, K. Ghosh, G. Velayutham, N. Rajalakshmi, et al., Int. J. Hydrogen Energy 24 (1999) 1107–1115.
[31] S. Giddey, F. Ciacchi, S. Badwal, J. Power Sources 125 (2004) 155–165.
[32] C. Bonnet, S. Didierjean, N. Guillet, S. Besse, T. Colinart, P. Carré, J. Power Sources 182 (2008) 441–448.
[33] F. Weng, B. Jou, A. Su, S.H. Chan, P. Chi, J. Power Sources 171 (2007) 179–185.
[34] L. Bonville, H. Kunz, Y. Song, A. Mientek, M. Williams, A. Ching, et al., J. Power Sources 144 (2005) 107–112.
[35] J. San Martin, I. Zamora, J. San Martin, V. Aperribay, E. Torres, P. Eguia, Energy 35 (2010) 1898–1907.
[36] C. Tori, M. Baleztena, C. Peralta, R. Calzada, E. Jorge, D. Barsellini, et al., Int. J. Hydrogen Energy 33 (2008) 3588–3591.
[37] M.H. Fronk, D. Wetter, D. Masten, A. Bosco, Proc. SAE 2000 World Congress, 2000.
[38] R. Eckl, W. Zehtner, C. Leu, U. Wagner, J. Power Sources 138 (2004) 137–144.
[39] J. Jang, H. Chiu, W. Yan, W. Sun, J. Power Sources 180 (2008) 476–483.
[40] Y. Park, J. Caton, J. Power Sources 179 (2008) 584–591.
[41] M. Perez-Page, V. Perez-Herranz, ECS Trans. 25 (2009) 733–745.
[42] F. Philipps, G. Simons, K. Schiefer, J. Power Sources 154 (2006) 412–419.
[43] G. Squadrito, O. Barbera, G. Giacoppo, F. Urbani, E. Passalacqua, J. Fuel Cell Sci. Technol. 4 (2007) 350–356.
[44] C. Wang, Z. Mao, F. Bao, X. Li, X. Xie, Int. J. Hydrogen Energy 30 (2005) 1031–1034.
[45] S. Ahn, S. Shin, H. Ha, S. Hong, Y. Lee, T. Lim, et al., J. Power Sources 106 (2002) 295–303.
[46] P. Pei, X. Yuan, P. Chao, X. Wang, Int. J. Hydrogen Energy 35 (2010) 3147–3151.
[47] T. Mennola, M. Mikkola, M. Noponen, T. Hottinen, P. Lund, J. Power Sources 112 (2002) 261–272.
[48] G. Tian, S. Wasterlain, I. Endichi, D. Candusso, F. Harel, X. François, et al., J. Power Sources 182 (2008) 449–461.
[49] M. Hu, S. Sui, X. Zhu, Q. Yu, G. Cao, X. Hong, et al., Int. J. Hydrogen Energy 31 (2006) 1010–1018.
[50] P. Moçotéguy, B. Ludwig, J. Scholta, R. Barrera, S. Ginocchio, Fuel Cells 9 (2009) 325–348.

[51] P. Moçotéguy, B. Ludwig, J. Scholta, Y. Nedellec, D. Jones, J. Rozière, Fuel Cells 10 (2010) 299–311.
[52] J. Scholta, N. Berg, P. Wilde, L. Jörissen, J. Garche, J. Power Sources 127 (2004) 206–212.
[53] H. Lee, C. Lee, T. Oh, S. Choi, I. Park, K. Baek, J. Power Sources 107 (2002) 110–119.
[54] Y. Matsushita, J. Okano, K. Okajima, ECS Trans. (2009) 181–190.
[55] J. Okano, Y. Matsushita, K. Okajima, ECS Trans. (2009) 141–150.
[56] D. Webb, S. Møller-Holst, J. Power Sources 103 (2001) 54–60.
[57] M. Hinaje, D. Nguyen, S. Raël, B. Davat, C. Bonnet, F. Lapicque, Int. J. Hydrogen Energy 34 (2009) 6364–6370.
[58] G. Tian, S. Wasterlain, D. Candusso, F. Harel, D. Hissel, X. François, Int. J. Hydrogen Energy 35 (2010) 2772–2776.
[59] S. Morner, S. Klein, J. Sol. Energy Eng. 123 (2001) 225–231.
[60] R.G. Fellows, Method and system for operating fuel cell stacks to reduce non-steady state conditions during load transients, n.d.
[61] C.A. Reiser, Method and apparatus for improved delivery of input reactants to a fuel cell assembly, US Patent 6,497,971 (2002).
[62] J.H. Whiton, Y. Wang, C.A. Reiser, G.S. Hirko, Small volume, fuel cell inlet fuel gas distributor having low pressure drop, n.d.
[63] J. Dong, Y. Zhou, Flow-field plate and fuel cell stack using the same, n.d.
[64] X. Chen, D. Frank, Fuel cell with dual end plate humidifiers, US Patent 6,602,625 (2003).
[65] D.R. Pedersen, K. Silberbauer, Fuel cell stack performance monitoring, n.d.
[66] S. Andreasen, J. Jespersen, E. Schaltz, S. Kær, Fuel Cells 9 (2009) 463–473.
[67] B. Wahdame, D. Candusso, X. François, F. Harel, M. Péra, D. Hissel, et al., Int. J. Hydrogen Energy 32 (2007) 4523–4536.
[68] B. Wahdame, D. Candusso, F. Harel, X. François, M. Péra, D. Hissel, et al., J. Power Sources 182 (2008) 429–440.
[69] X. Yan, M. Hou, L. Sun, D. Liang, Q. Shen, H. Xu, et al., Int. J. Hydrogen Energy 32 (2007) 4358–4364.
[70] Q. Yan, H. Toghiani, H. Causey, J. Power Sources 161 (2006) 492–502.
[71] T. Isono, S. Suzuki, M. Kaneko, Y. Akiyama, Y. Miyake, I. Yonezu, J. Power Sources 86 (2000) 269–273.
[72] S. Knights, K. Colbow, J. St-Pierre, D. Wilkinson, J. Power Sources 127 (2004) 127–134.
[73] F. Laurencelle, R. Chahine, J. Hamelin, K. Agbossou, M. Fournier, T. Bose, Fuel Cells 1 (2001) 66–71.
[74] K. Adegnon, Y. Dubé, K. Agbossou, Proc. Canadian Conference on Electrical and Computer Engineering, 2009, pp. 716–719.
[75] P. Corbo, F. Migliardini, O. Veneri, Int. J. Hydrogen Energy 32 (2007) 4340–4349.
[76] D. Chu, R. Jiang, J. Power Sources 83 (1999) 128–133.
[77] G. Jung, K. Lo, A. Su, F. Weng, C. Tu, T. Yang, et al., Int. J. Hydrogen Energy 33 (2008) 2980–2985.
[78] S. Lee, I. Min, H. Kim, S.W. Nam, J. Lee, S.J. Kim, et al., J. Fuel Cell Sci. Technol. 7 (2010) 031006–31007.
[79] B. Wahdame, D. Candusso, X. François, F. Harel, A. De Bernardinis, J. Kauffmann, et al., Fuel Cells 7 (2007) 47–62.
[80] X. Yuan, J. Sun, M. Blanco, H. Wang, J. Zhang, D. Wilkinson, J. Power Sources 161 (2006) 920–928.
[81] K. Choi, H. Kim, H. Yoon, M. Forrest, P. Erickson, Energy Convers. Manag. 49 (2008) 3505–3511.
[82] C. Brunetto, A. Moschetto, G. Tina, Electr. Power Syst. Res. 79 (2009) 17–26.
[83] P. Corbo, F. Migliardini, O. Veneri, Energy Convers. Manag. 48 (2007) 2365–2374.
[84] L. Lu, M. Ouyang, H. Huang, P. Pei, F. Yang, J. Power Sources 164 (2007) 306–314.
[85] P.J. Ferreira, J. Electrochem. Soc. 152 (2005) A2256–A2271.
[86] J. Wu, X. Yuan, J. Martin, H. Wang, D. Yang, J. Qiao, et al., J. Power Sources 195 (2010) 1171–1176.
[87] Z. Luo, D. Li, H. Tang, M. Pan, R. Ruan, Int. J. Hydrogen Energy 31 (2006) 1831–1837.
[88] X. Yuan, S. Zhang, H. Wang, J. Wu, J.C. Sun, R. Hiesgen, et al., J. Power Sources 195 (2010) 7594–7599.
[89] J. Wu, X. Yuan, H. Wang, M. Blanco, J. Martin, J. Zhang, Int. J. Hydrogen Energy 33 (2008) 1735–1746.
[90] F. Ettingshausen, J. Kleemann, M. Michel, M. Quintus, H. Fuess, C. Roth, J. Power Sources 194 (2009) 899–907.
[91] X. Yuan, H. Wang, J. Colin Sun, J. Zhang, Int. J. Hydrogen Energy 32 (2007) 4365–4380.
[92] M. Ciureanu, J. Appl. Electrochem. 34 (2004) 705–714.
[93] A. Hakenjos, M. Zobel, J. Clausnitzer, C. Hebling, J. Power Sources 154 (2006) 360–363.
[94] J. Le Canut, R. Abouatallah, D. Harrington, J. Electrochem. Soc. 153 (2006) A857–A864.
[95] W. Zhu, R. Payne, B. Tatarchuk, J. Power Sources 168 (2007) 211–217.
[96] J. Diard, N. Glandut, B. Le Gorrec, C. Montella, J. Electrochem. Soc. 151 (2004) A2193–A2197.
[97] B. Chiem, P. Beattie, K. Colbow, ECS Trans. (2008) 1927–1935.
[98] P. Lehman, C. Chamberlin, G. Chapman, N. Coleman, R. Engel, D. McKay, et al., Proc. Fuel Cell Seminar, Palm Springs, CA, 2002.
[99] S. Zhang, H. Yu, H. Zhu, J. Hou, B. Yi, P. Ming, Chin. J. Chem. Eng. 14 (2006) 802–805.
[100] P. Lehman, C. Chamberlin, J. Zoellick, R. Engel, D. Rommel, Proc. 14th World Hydrogen Energy Conference, 2002.
[101] M. Scagliotti, C. Valli, J. Fuel Cell Sci. Technol. 7 (2010) 031014-9.
[102] J. St-Pierre, N. Jia, J. New Mater. Electrochem. Syst. 5 (2002) 263–271.
[103] J. Li, K. Wang, Y. Yang, ECS Trans. 25 (2009) 385–394.
[104] M. Ferraro, F. Sergi, G. Brunaccini, G. Dispenza, L. Andaloro, V. Antonucci, J. Power Sources 193 (2009) 342–348.
[105] G. Lee, M. Jung, S. Ryoo, M. Park, S. Ha, S. Kim, Int. J. Hydrogen Energy, in press, Corrected Proof (n.d.), doi:10.1016/j.ijhydene.2010.04.081.
[106] S. Yoshioka, A. Yoshimura, H. Fukumoto, O. Hiroi, H. Yoshiyasu, J. Power Sources 144 (2005) 146–151.
[107] J. Chen, B. Zhou, J. Power Sources 177 (2008) 83–95.
[108] R. Alink, D. Gerteisen, M. Oszcipok, J. Power Sources 182 (2008) 175–187.
[109] W. Schmittinger, A. Vahidi, J. Power Sources 180 (2008) 1–14.
[110] S. Philipps, C. Ziegler, J. Power Sources 180 (2008) 309–321.
[111] S. Andreasen, S. Kær, Int. J. Hydrogen Energy 33 (2008) 4655–4664.
[112] G. Bucci, F. Ciancetta, E. Fiorucci, E. Rotondale, F. Vegliò, Proc. International Symposium on Power Electronics, Electrical Drives, Automation and Motion, 2006, pp. 546–551.
[113] J. Hamelin, K. Agbossou, A. Laperrière, F. Laurencelle, T. Bose, Int. J. Hydrogen Energy 26 (2001) 625–629.
[114] P. Schiavetti, Z. Del Prete, Rev. Sci. Instrum. 78 (2007).
[115] X. Zhu, D. Xu, P. Wu, G. Shen, P. Chen, Proc. IEEE Applied Power Electronics Conference and Exposition (APEC), 2008, pp. 291–297.
[116] D. Chrenko, M. Péra, D. Hissel, M. Geweke, J. Fuel Cell Sci. Technol. 5 (2008).
[117] A. del Real, A. Arce, C. Bordons, J. Power Sources 173 (2007) 310–324.
[118] H. Kim, C. Cho, J. Nam, D. Shin, T. Chung, Int. J. Hydrogen Energy 35 (2010) 3656–3663.
[119] Y. Tang, W. Yuan, M. Pan, Z. Li, G. Chen, Y. Li, Appl. Energy 87 (2010) 1410–1417.
[120] P. Corbo, F. Migliardini, O. Veneri, Renew. Energy 34 (2009) 1955–1961.
[121] P. Corbo, F. Migliardini, O. Veneri, Energy Convers. Manag. 49 (2008) 2688–2697.
[122] M. Khandelwal, J. Ko, M. Mench, ECS Trans. (2007) 553–563.
[123] M. Oszcipok, M. Zedda, D. Riemann, D. Geckeler, J. Power Sources 154 (2006) 404–411.
[124] E. Schießwohl, T. von Unwerth, F. Seyfried, D. Brüggemann, J. Power Sources 193 (2009) 107–115.
[125] S. Bégot, F. Harel, J.M. Kauffmann, Fuel Cells 8 (2008) 138–150.
[126] U. Limbeck, Fuel cell system with improved cold start properties and method, US Patent WO/2008/148445 (2008).
[127] A.E. Nelson, Method of starting up fuel cell stacks from freezing temperatures, US Patent WO/2008/118962 (2008).
[128] C.A. Reiser, G. Resnick, System and method for starting a fuel cell stack assembly at sub-freezing temperature, US Patent 7,056,609 (2006).
[129] R.D. Breault, P.L. Hagans, Method of operating a fuel cell system under freezing conditions, US Patent 7,049,018 (2006).
[130] E.L. Thompson, R.L. Fuss, Control system and method for starting a frozen fuel cell, US Patent 6,887,598 (2005).
[131] C.A. Reiser, F.F. Sribnik, Fuel cell stack melting of coolant water during frozen startup, US Patent 6,986,958 (2006).
[132] M. Inaba, ECS Trans. 25 (2009) 573–581.
[133] J. Nordlund, A. Ocklind, P. Gode, Proc. INTELEC, International Telecommunications Energy Conference, 2008.
[134] A. Ocklind, J. Nordlund, Newsl.: Fuel Cells 1/09 (2009) 1.
[135] J. Marcinkoski, J.P. Kopasz, T.G. Benjamin, Int. J. Hydrogen Energy 33 (2008) 3894–3902.
[136] N. Myers, J. DeHaan, Proc. Battcon Conference, Miami Beach, FL, 2005.
[137] S. Saathoff, Fuel Cells Bull. 2004 (2004) 10–12.
[138] H. Chang, C. Chou, Y. Chen, T. Hou, B. Weng, Int. J. Hydrogen Energy 32 (2007) 316–322.
[139] M.L. Perry, E. Strayer, Proc. INTELEC, International Telecommunications Energy Conference, 2006, pp. 1–8.
[140] A. Tomasi, R. Marin, Proc. INTELEC, International Telecommunications Energy Conference, 2007, pp. 116–121.
[141] A. Tomasi, M. Concina, M. Grossoni, P. Caracino, J. Blanchard, Proc. INTELEC, International Telecommunications Energy Conference, 2006.
[142] A. Tomasi, A. Torelli, G. Calzetti, Proc. INTELEC, International Telecommunications Energy Conference, 2007, pp. 122–125.
[143] A. Torrelli, G. Calzetti, A. Orlando, P. Magnanini, G. Gagliardi, Proc. INTELEC, International Telecommunications Energy Conference, 2007, pp. 108–115.
[144] G. Gianolio, I. Rosso, P. Cherchi, F. Pedrazzo, A. Torrelli, G. Calzetti, et al., Proc. INTELEC, International Telecommunications Energy Conference, 2007, pp. 280–287.
[145] A. Trehan, D. Canavan, Proc. INTELEC, International Telecommunications Energy Conference, 2008.
[146] J. Blanchard, Proc. INTELEC, International Telecommunications Energy Conference, 2007, pp. 563–567.
[147] D. Canavan, J. Dogterom, J. McDougall, Proc. INTELEC, International Telecommunications Energy Conference, 2006.
[148] M. Saxe, A. Folkesson, P. Alvfors, Energy 33 (2008) 689–711.
[149] K. Haraldsson, A. Folkesson, P. Alvfors, J. Power Sources 145 (2005) 620–631.
[150] X. Li, J. Li, L. Xu, F. Yang, J. Hua, M. Ouyang, Int. J. Hydrogen Energy 35 (2010) 3841–3847.
[151] K. Bonhoff, J. Power Sources 181 (2008) 350–352.
[152] S. Romano, J. Larkins, Fuel Cells 3 (2003) 128–132.

[153] P. Bubna, D. Brunner, J.J. Gangloff Jr., S.G. Advani, A.K. Prasad, J. Power Sources 195 (2010) 3939–3949.
[154] K. Chandler, L. Eudy, Santa Clara Valley Transportation Authority and San Mateo County Transit District Fuel Cell Transit Buses: Evaluation Results, National Renewable Energy Laboratory, 2006.
[155] K. Chandler, L. Eudy, Alameda-Contra Costa Transit District (AC Transit) Fuel Cell Transit Buses: Third Evaluation Report, National Renewable Energy Laboratory, 2008.
[156] K. Chandler, L. Eudy, Connecticut Transit (CTTRANSIT) Fuel Cell Transit Bus: Second Evaluation Report, National Renewable Energy Laboratory, 2009.
[157] L. Eudy, K. Chandler, National Renewable Energy Laboratory (2007).
[158] L. Eudy, K. Chandler, SunLine Transit Agency Fuel Cell Transit Bus: Fifth Evaluation Report, National Renewable Energy Laboratory, 2009.
[159] G. Friedlmeier, J. Friedrich, F. Panik, Fuel Cells 1 (2001) 92–96.
[160] A. Feitelberg, J. Stathopoulos, Z. Qi, C. Smith, J. Elter, J. Power Sources 147 (2005) 203–207.
[161] G. Gigliucci, L. Petruzzi, E. Cerelli, A. Garzisi, A. La Mendola, J. Power Sources 131 (2004) 62–68.
[162] A. Maekawa, T. Aoki, ECS Trans. (2005) 385–400.
[163] M. Pokojski, J. Power Sources 86 (2000) 140–144.
[164] W. Münch, H. Frey, M. Edel, A. Kessler, J. Power Sources 155 (2006) 77–82.
[165] N. Kato, K. Uchimoto, K. Kudo, T. Sakai, N. Makita, M. Murai, et al., Proc. INTELEC, International Telecommunications Energy Conference, 2003, pp. 77–83.
[166] M. Rissanen, G. Bark, E. Lindman, ECS Trans. (2007) 835–841.
[167] A. Chaparro, J. Soler, M. Escudero, E. de Ceballos, U. Wittstadt, L. Daza, J. Power Sources 144 (2005) 165–169.
[168] J. Hwang, M. Zou, J. Power Sources 195 (2010) 2579–2585.
[169] M. Davis, A. Fanney, M. LaBarre, K. Henderson, B. Dougherty, J. Fuel Cell Sci. Technol. 4 (2007) 109–115.
[170] R. Clarke, S. Giddey, F. Ciacchi, S. Badwal, B. Paul, J. Andrews, Int. J. Hydrogen Energy 34 (2009) 2531–2542.
[171] N.A. Freeman, S. Masse, R.B. Gopal, System and method for measuring FC voltage and high frequency resistance, US Patent 2,477,465 (n.d.).
[172] P. Coenen, System and method for measuring fuel cell voltage, n.d.
[173] N.V. Dale, M.D. Mann, H. Salehfar, A.M. Dhirde, T. Han, J. Fuel Cell Sci. Technol. 7 (2010) 031010-10.
[174] O. Yamazaki, H. Shintaku, Y. Oomori, T. Tabata, ECS Trans. 16 (2008) 1967–1975.
[175] P. Pei, M. Ouyang, W. Feng, L. Lu, H. Huang, J. Zhang, Int. J. Hydrogen Energy 31 (2006) 371–377.
[176] S. Motupally, C.A. Reiser, Method for minimizing membrane electrode degradation in a fuel cell power plant, n.d.
[177] S. Lux, M. Binder, F. Holcomb, N. Josefik, Fuel Cells Bull. 2003 (2003) 11–15.
[178] H. Onovwiona, V. Ugursal, Energy Rev. 10 (2006) 389–431.
[179] J.E. Brown, C.N. Hendry, P. Harborne, Energy Policy 35 (2007) 2173–2186.
[180] B. Du, Q. Guo, R. Pollard, D. Rodriguez, C. Smith, J. Elter, J. Miner. Met. Mater. Soc. 58 (2006) 45–49.
[181] F. de Brujin, Green Chem. 7 (2005) 132–150.